

Electronic Supplementary Information for

The Tetracyanoborate Anion as Building Block for the Heterocubane Cluster Cage $[\text{Cr}_4\text{B}_4(\text{CN})_{16}]^{4-}$

Martin S. Luff^[a], Rüdiger Bertermann^[a,b], Maik Finze^{*[a,b]}, Udo Radius^{*[a]}

[a] Institute for Inorganic Chemistry, Julius-Maximilians-Universität Würzburg, Am Hubland, 97074 Würzburg, Germany.

[b] Institute for Sustainable Chemistry & Catalysis with Boron, Julius-Maximilians-Universität Würzburg, Am Hubland, 97074 Würzburg, Germany.

*Corresponding author Email address: u.radius@uni-wuerzburg.de, maik.finze@uni-wuerzburg.de

1	Additional Figures and Tables	2
2	Experimental Section.....	8
2.1	General Information	8
2.2	Experimental Details	8
3	NMR Spectroscopy Section	10
3.1	General Information	10
3.2	NMR Spectra	10
4	Infrared and Raman Spectroscopy Section	14
4.1	General Information	14
4.2	IR and Raman Spectra	14
5	Crystallographic Information	17
5.1	General Information	17
5.2	Crystallographic Data.....	18
6	Author Contributions	24
7	References.....	24

1 Additional Figures and Tables

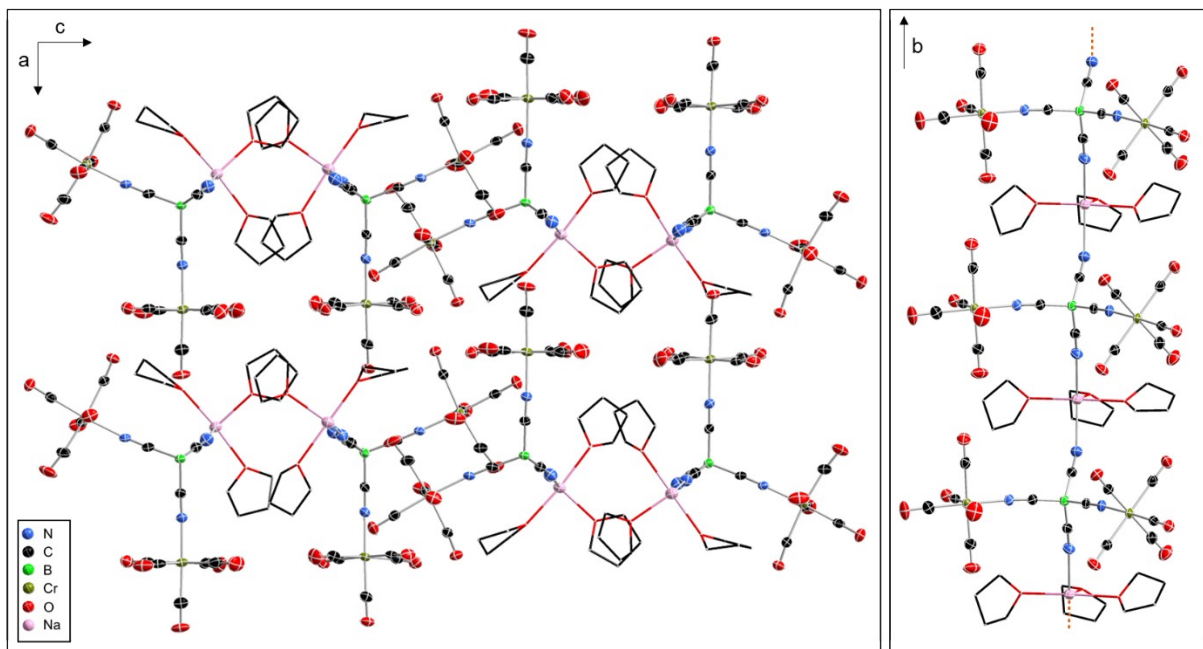


Figure S1. The coordination polymer $^1\{\infty\{\text{Na}(\text{THF})_3[\text{Cr}(\text{CO})_5(\text{B}(\text{CN})_4\text{Cr}(\text{CO})_5]\}\}$ ($^1\{\infty\{\text{Na}(\text{THF})_3[2]\}\}$) (ellipsoids set at 50% probability level). Left: Unit cell of $^1\{\infty\{\text{Na}(\text{THF})_3[2]\}\}$ viewed along the b-axis at the a-c-plane showing eight distinct monomers of different polymeric strands. Right: Polymeric strand of $^1\{\infty\{\text{Na}(\text{THF})_3[2]\}\}$ with three monomers with perspective orthogonal to the b-axis. Selected bond lengths and angles are given in the figure captions of Figure S17. The hydrogen atoms are omitted for clarity.

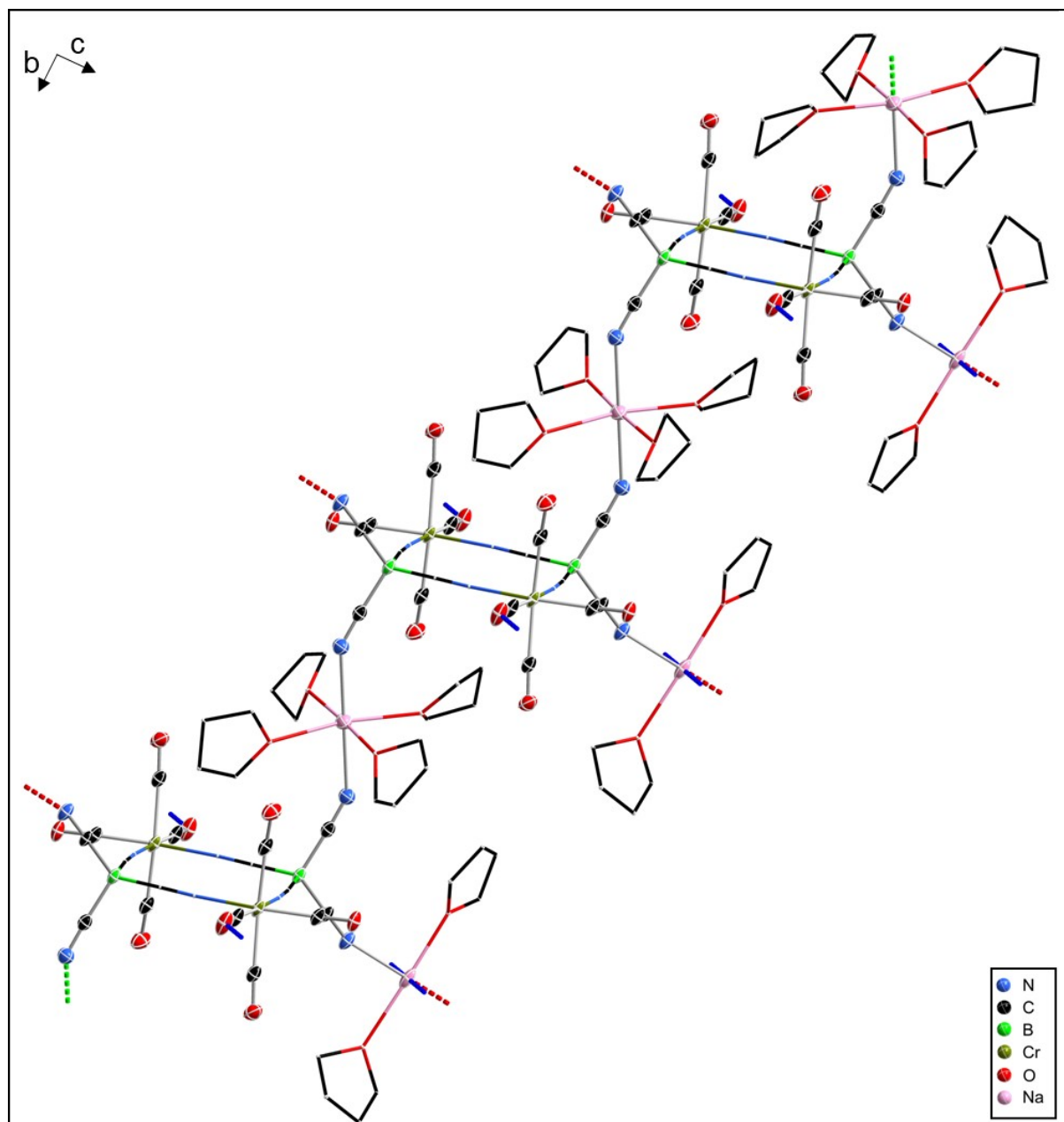


Figure S2. The coordination polymer $\text{Na}_2(\text{THF})_6[\{\text{Cr}(\text{CO})_4(\text{B}(\text{CN})_4)\}_2]\cdot 2\text{THF}$ ($\text{Na}_2(\text{THF})_6[\text{5}]\cdot 2\text{THF}$) in the solid-state (ellipsoids set at 50% probability level). Selected bond lengths and angles are given in the figure captions of Figure S18. The hydrogen atoms are omitted for clarity.

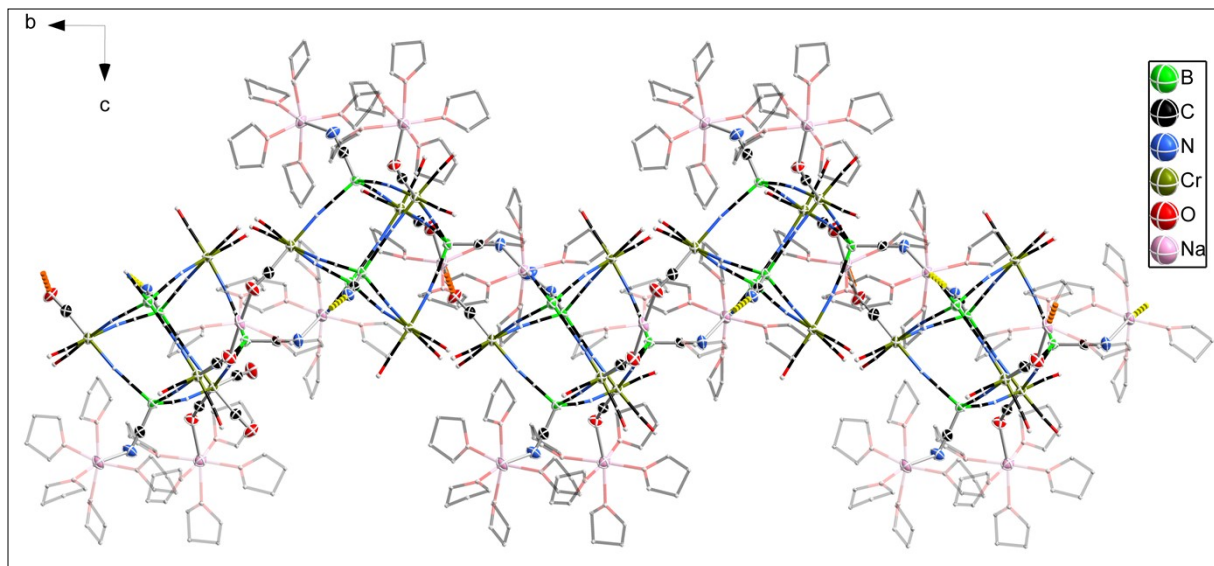


Figure S3A. The coordination polymer $\infty\{\text{Na}_4(\text{THF})_{17}[\{\text{Cr}(\text{CO})_3(\text{B}(\text{CN})_4)\}_4]\}\cdot 2\text{THF}$ ($\infty\{\text{Na}_4(\text{THF})_{17}[6]\}\cdot 2\text{THF}$) in the solid-state (ellipsoids set at 50% probability level; Perspective along the a-axis). Selected bond lengths and angles are given in the figure captions of Figure S19. The hydrogen atoms are omitted for clarity.

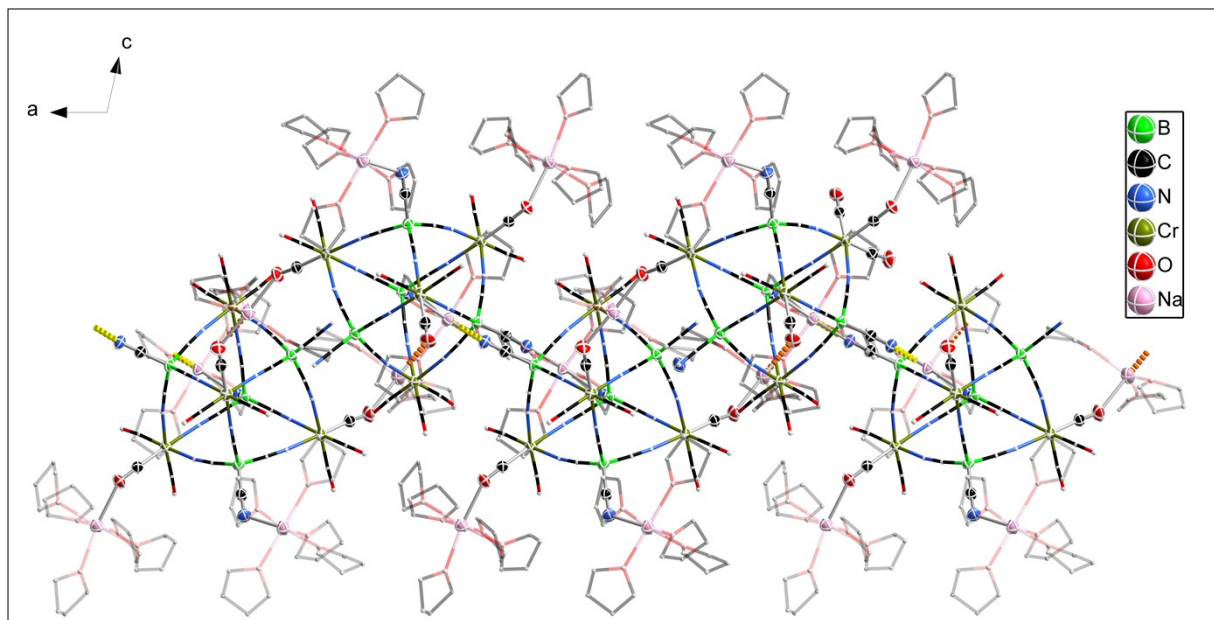


Figure S3B. The coordination polymer $\infty\{\text{Na}_4(\text{THF})_{17}[\{\text{Cr}(\text{CO})_3(\text{B}(\text{CN})_4)\}_4]\}\cdot 2\text{THF}$ ($\infty\{\text{Na}_4(\text{THF})_{17}[6]\}\cdot 2\text{THF}$) in the solid-state (ellipsoids set at 50% probability level; Perspective along the b-axis). Selected bond lengths and angles are given in the figure captions of Figure S19. The hydrogen atoms are omitted for clarity.

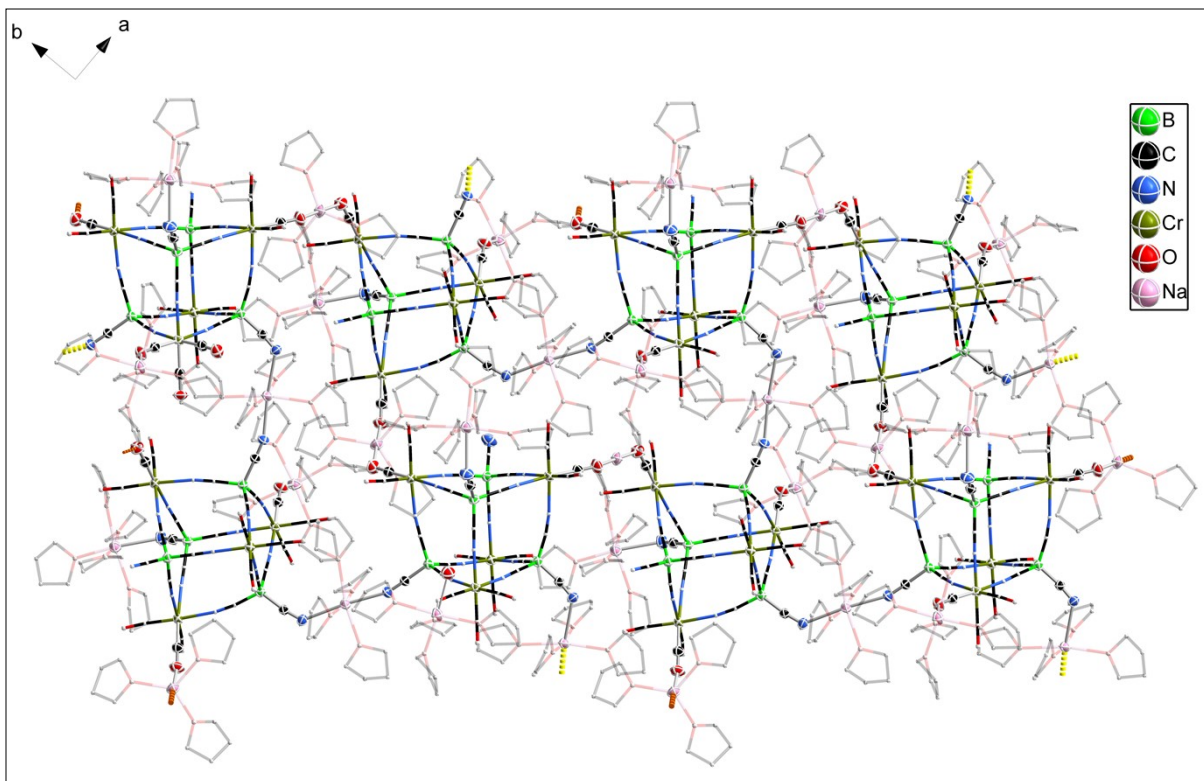


Figure S3C. The coordination polymer $\text{Na}_4(\text{THF})_{17}[\{\text{Cr}(\text{CO})_3(\text{B}(\text{CN})_4)\}_4]\cdot 2\text{THF}$ ($\infty\{\text{Na}_4(\text{THF})_{17}[6]\}\cdot 2\text{THF}$) in the solid-state (ellipsoids set at 50% probability level; Perspective along the c-axis). Selected bond lengths and angles are given in the figure captions of Figure S19. The hydrogen atoms are omitted for clarity.

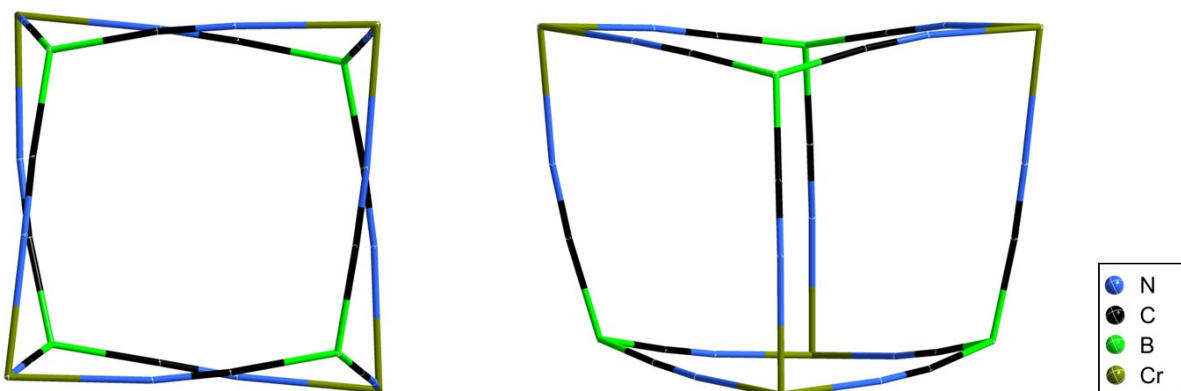


Figure S4. Wireframe model of the $[\text{Cr}_4\{\text{B}(\text{CN})_3\}_4]$ framework in $\infty\{\text{Na}_4(\text{THF})_{17}[6]\}\cdot 2\text{THF}$.

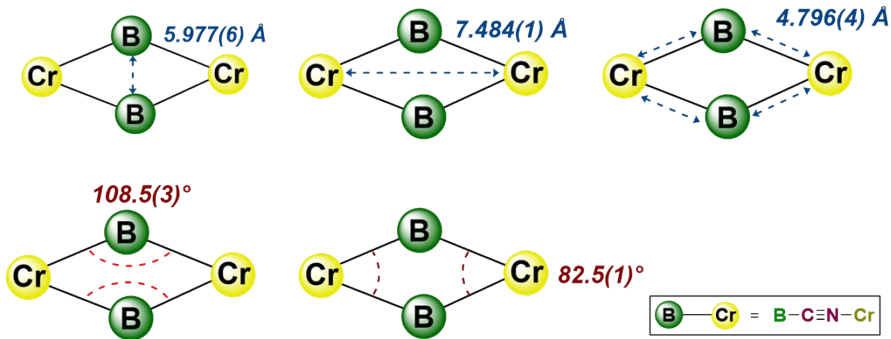


Figure S5. Schematic representation of the rectangular frame of $\{[\text{Cr}(\text{CO})_4(\text{NC}-\text{B}(\text{CN})_2-\text{CN})\}_2\}^{2-}$ (**5**) and relevant bond distances and bond angles.

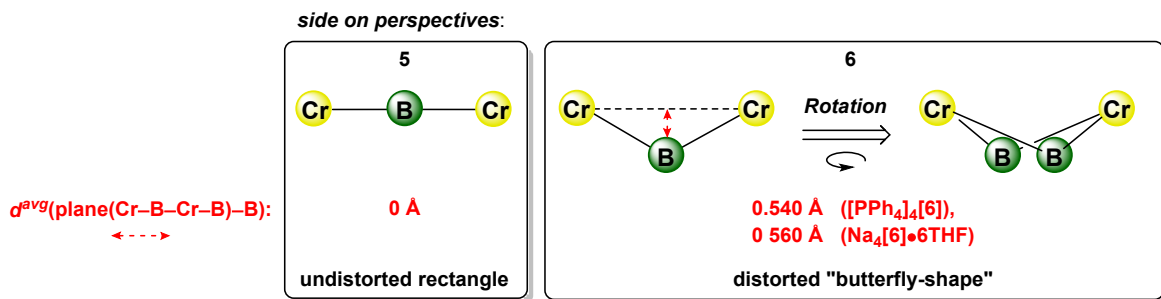


Figure S6. Schematic representation of the distortion from the rectangular shape of $\text{K}_2[\text{Cr}(\text{CO})_4(\text{NC}-\text{B}(\text{CN})_2-\text{CN})]$ (**K₂[5]**) and the distorted, „butterfly-shape“ in $[\text{Cat}]_4[\{\text{Cr}(\text{CO})_3(\text{B}(\text{CN})_4)\}_4]\cdot x\text{THF}$ (**[Cat]₄[6]**; Cat = PPh_4 ; Cat = Na), as well as average distances of the boron atoms to the plane(Cr-B-Cr-B). Dashed line represents the plane(Cr-B-Cr-B).

Table S1. Selected average experimental bond lengths [\AA] and angles [$^\circ$] of the synthesized cyanoborate chromium complexes. Non-averaged bond lengths and angles are given in Table S2.

Compound	d^{avg} (Cr-CO)	d^{avg} (Cr-NC)	d^{avg} (Na-NC)	d^{avg} (Cr-B)	d^{avg} (B-B)	d^{avg} (Cr-Cr)	α^{avg} (N-Cr-N)	α^{avg} (NC-B-CN)	d^{avg} (plane(Cr-B-Cr-B)-B))
${}^1_{\infty}\{\text{Na}_2(\text{THF})_3[\{\text{Cr}(\text{CO})_5-\text{NC}_2(\text{B}(\text{CN})_2)\}]\cdot {}^1_{\infty}\text{Na}(\text{THF})_3[2]\}$	1.856, ^a 1.911	2.060	2.445	4.788	—	7.973(1)	—	110.2(3)	—
${}^3_{\infty}\{\text{Na}_2(\text{THF})_6[\{\text{Cr}(\text{CO})_4(\text{B}(\text{CN})_4)\}_2]\}\cdot 2\text{THF}$ $({}^3_{\infty}\text{Na}_2(\text{THF})_6[5])\cdot 2\text{THF}$	1.853(4) ^a 1.830(4) ^{b,c} 1.913	2.063	2.443	4.796(4)	5.977(6)	7.484(1)	82.5(1)	108.5(3)	0
${}^2_{\infty}\{\text{Na}_4(\text{THF})_{17}[\{\text{Cr}(\text{CO})_3(\text{B}(\text{CN})_4)\}_4]\}\cdot 2\text{THF}$ $({}^2_{\infty}\text{Na}_4(\text{THF})_{17}[6])\cdot 2\text{THF}$	1.816, ^b 1.834	2.073	2.452	4.795	5.871	7.497	82.9	108.4	0.560
$[\text{PPh}_4]_4[\{\text{Cr}(\text{CO})_3(\text{B}(\text{CN})_4)\}_4]\cdot 7.5\text{THF}$ $([\text{PPh}_4]_4[6]\cdot 7.5\text{THF})$	1.833	2.076	—	4.799	5.923	7.474	83.3	108.2	0.540

^a Data concerning equatorial (*trans*- relative to CB) coordinated CO groups. ^b Data concerning Na^+ coordinated CO groups.

Table S2. Selected experimental bond lengths [\AA] and angles [°] of the synthesized cyanoborate chromium complexes. Averaged bond lengths and angles are given in Table S1.

Compound	$d(\text{Cr}-\text{CO})$	$d(\text{Cr}-\text{NC})$	$d(\text{Na}-\text{NC})$	$d(\text{Cr}-\text{B})$	$d(\text{B}-\text{B})$	$d(\text{Cr}-\text{Cr})$	$\angle \text{N}-\text{Cr}-\text{N}$	$\angle \text{NC}-\text{B}-\text{CN}$	d^{avg} (plane($\text{Cr}-\text{B}-\text{Cr}-\text{B}$))
${}^1_{\omega}\{\text{Na}(\text{THF})_3[\{\text{Cr}(\text{CO})_3-\text{NC}\}_2(\text{B}(\text{CN})_2)\}$ $({}^1_{\omega}\{\text{Na}(\text{THF})_3[2]\})$	1.860(4), ^a 1.908(4), 1.915(5), 1.925(5), 1.903(5), 1.852(5), [*] 1.917(4), 1.894(5), 1.917(4), 1.911(4)	2.066(3), 2.054(4)	2.434(4), 2.456(4)	4.800(4), 4.775(4)	—	7.973(1)	—	110.2(3)	—
${}^3_{\omega}\{\text{Na}_2(\text{THF})_3[\{\text{Cr}(\text{CO})_3(\text{B}(\text{CN})_4)\}_2]\}$ $\cdot 2\text{THF}$ $({}^3_{\omega}\{\text{Na}_2(\text{THF})_3[5]\}\cdot 2\text{THF})$	1.853(5), ^a 1.830(1), ^a 1.898(4), 1.927(4)	2.062(3), 2.064(3)	2.430(3), 2.456(3)	4.796(4)	5.977(6)	7.484(1)	82.5(1)	108.5(3)	0
${}^2_{\omega}\{\text{Na}_4(\text{THF})_7[\{\text{Cr}(\text{CO})_3(\text{B}(\text{CN})_4)\}_4]\}$ $\cdot 2\text{THF}$ $({}^2_{\omega}\{\text{Na}_4(\text{THF})_7[6]\}\cdot 2\text{THF})$	1.845(4), 1.827(5), 1.833(4), 1.830(4), 1.832(4), 1.826(4), 1.831(4), 1.836(4), 1.842(4), 1.817(4), ^b 1.811(4), ^b 1.819(4), ^b	2.083(3), 2.076(3), 2.081(3), 2.064(3), 2.068(3), 2.072(3), 2.063(3), 2.062(3), 2.075(3), 2.078(3), 2.068(4), 2.083(3)	2.360(3), 2.469(4), 2.435(3), 2.543(4)	4.801(4), 4.772(4), 4.791(4), 4.803(4), 4.801(4), 4.805(4), 4.796(4), 4.801(4), 4.778(4), 4.812(4), 4.787(4), 4.794(4)	5.820(5), 5.875(6), 5.873(6), 5.916(5), 5.916(5), 5.798(6)	7.497(1), 7.506(1), 7.536(1), 7.535(1), 7.460(1), 7.448(1)	83.7(1), 83.3(1), 82.2(1), 82.7(1), 83.1(1), 82.2(1), 83.9(1), 83.1(1), 83.3(1), 81.9(1), 82.8(1), 82.3(1)	108.9(3), 107.4(3), 108.6(3), 108.5(3), 108.1(3), 108.7(3), 107.5(3), 108.0(3), 108.8(3), 108.6(3), 109.3(3), 108.9(3)	0.600(4), 0.585(4), 0.581(4), 0.563(4), 0.548(4), 0.511(4), 0.598(4), 0.513(4), 0.542(4), 0.519(4), 0.581(4), 0.581(4)
$[\text{PPh}_4]_4[\{\text{Cr}(\text{CO})_3(\text{B}(\text{CN})_4)\}_4]$ $\cdot 7.5\text{THF}$ $([\text{PPh}_4]_4[6]\cdot 7.5\text{THF})$	1.834(4), 1.836(4), 1.838(4), 1.841(4), 1.829(4), 1.830(4), 1.820(4), 1.846(4), 1.824(4), 1.830(5), 1.831(4), 1.834(4)	2.072(3), 2.093(3), 2.080(3), 2.067(3), 2.076(3), 2.084(3), 2.072(3), 2.067(3), 2.079(3), 2.064(3), 2.063(3), 2.090(3)	—	4.798(4), 4.801(4), 4.783(5), 4.803(4), 4.801(4), 4.786(4), 4.805(4), 4.801(4), 4.798(4), 4.786(4), 4.809(5), 4.813(4)	5.916(4), 6.021(6), 5.910(6), 5.865(6), 5.912(6), 5.916(4)	7.371(9), 7.479(6), 7.510(9), 7.478(8), 7.528(1), 82.7(1), 82.7(1), 83.4(1), 83.4(1), 82.5(1), 84.0(1), 82.5(1)	83.0(1), 84.9(1), 83.3(1), 83.0(1), 84.3(1), 82.7(1), 82.7(1), 83.4(1), 83.4(1), 82.5(1), 84.0(1), 82.5(1)	107.9(3), 108.9(3), 108.5(3), 106.4(3), 108.2(3), 108.5(3), 108.5(3), 108.5(3), 108.5(3), 107.8(3), 108.7(3), 108.2(3)	0.493(3), 0.534(4), 0.580(4), 0.575(4), 0.539(5), 0.537(5), 0.633(4), 0.541(4), 0.707(5), 0.352(4), 0.492(4), 0.494(4)

^a Marked data concerning equatorial (*trans*- relative to CB) coordinated CO groups. ^b Data concerning Na⁺ coordinated CO groups.

Table S3. Selected NMR (ppm), IR and Raman (cm⁻¹) spectroscopic data of sodium and phosphonium salts of **6**.

Compound	$\delta^{(11)\text{B}}$	$\delta^{(13)\text{C}}\text{CO}$	$\delta^{(13)\text{C}}\text{CN}$	$\delta^{(23)\text{Na}}$	$\delta^{(31)\text{P}}$	$\nu(\text{CN})$	$\nu_1(\text{CO})$	$\nu_2(\text{CO})$
$\text{Na}_4[\text{Cr}(\text{CO})_3(\text{B}(\text{CN})_4)_4]\cdot 6\text{THF}$ $(\text{Na}_4[6]\cdot 6\text{THF})$	-37.1	236.3–222.3	125.8, 121.4	-14.9	—	2235, ^a 2239, ^b 2233 ^b	1912, ^a 1933, ^b	1797, ^a 1752 ^a
$[\text{PPh}_4]_4[\{\text{Cr}(\text{CO})_3(\text{B}(\text{CN})_4)_4\}]$ $([\text{PPh}_4]_4[6])$	-37.3	229.3	126.9	—	23.5	2224, ^a 2232, ^b 2223 ^b	1907, ^a 1929, ^a 1913 ^a	1779, ^a 1821 ^a

^a IR spectroscopical data. ^b Raman spectroscopical data.

2 Experimental Section

2.1 General Information

All reactions and subsequent manipulations involving organometallic reagents were performed under argon atmosphere by using standard Schlenk techniques or in a Glovebox (Innovative Technology Inc. and MBraun Uni Lab) as reported previously.¹ All reactions were carried out in oven-dried glassware. THF and *n*-hexane were obtained from a solvent purification station (Innovative Technology) by previous purification through alumina columns and then freshly distilled from sodium as a drying agent with benzophenone as an indicator. The deuterated solvents were purchased from Sigma-Aldrich and dried thoroughly over molecular sieves. The compounds Na[B(CN)₄],² [PPh₄][B(CN)₄],³ *fac*-[Cr(CO)₃(MeCN)₃],⁴ were synthesized according to known procedures. Elemental analyses were performed in the microanalytical laboratory of the University of Würzburg with an Elementar Vario Micro Cube.

2.2 Experimental Details

Crystallization of Na[{Cr(CO)₅-NC}₂B(CN)₂] (Na[2]) and Na₂[{Cr(CO)₄(B(CN)₄)₂}] (Na₂[5])

Solutions of [Cr(CO)₆] and Na[B(CN)₄] (*ca.* 50–200 mg scale) of varying stoichiometry of 1:1 to 4:1 in THF (10 mL) were irradiated with UV light for 24–120 h. The solvents were removed *in vacuo* and the residues washed with benzene (3 x 10 mL). The residues were extracted with THF or DME (5 mL) and *n*-hexane was diffused into these solutions over the course of several days, inducing crystallization of the yellow products. The compounds were obtained as the coordination polymers $\text{\textsupscript{1}}\{\text{Na}(\text{THF})_3[\text{Cr}(\text{CO})_5-\text{NC}]_2\text{B}(\text{CN})_2\}$ ($\text{\textsupscript{1}}\{\text{Na}(\text{THF})_3[2]\}$) and $\text{\textsupscript{3}}\{\text{Na}_2(\text{THF})_6[\{\text{Cr}(\text{CO})_4(\text{B}(\text{CN})_4)\}_2]\}\cdot 2\text{THF}$ ($\text{\textsupscript{3}}\{\text{Na}_2(\text{THF})_6[5]\}\cdot 2\text{THF}$). No yield was determined as only a few single-crystals were obtained. The compounds were not further characterized and the same products were obtained when the reaction mixtures were subjected to crystallization directly out of the reaction mixture without removal of the volatiles *in vacuo* and execution of the consequent washing step, which was carried out to remove most of the excess [Cr(CO)₆].

Synthesis of Na₄[{Cr(CO)₃(B(CN)₄)₄}] \cdot 6THF (Na₄[6] \cdot 6THF)

A solution of *fac*-[Cr(CO)₃(MeCN)₃] (150.0 mg, 578.7 μ mol, 1.0 eq.) in THF (5 mL) was treated with a solution of Na[B(CN)₄] (79.8 mg, 578.7 μ mol, 1.0 eq.) in THF (5 mL) and stirred for 4 hours. The crystalline precipitate was collected by filtration and washed with THF (3 x 5 mL) to produce Na₄[{Cr(CO)₃(B(CN)₄)₄}] \cdot 6THF (Na₄[6] \cdot 6THF) as a yellow solid. Single-crystals

suitable for X-ray structure determination were obtained directly out of the reaction mixture when no stirring was applied. **Yield:** 78% (173.0 mg, 113.2 μ mol). **Elemental analysis:** C₅₂H₄₈B₄Cr₄N₁₆Na₄O₁₈ [1528.23 g/mol] found (calc.): C 40.72 (40.87), H 3.12 (3.17), N 14.82 (13.61)%. **¹¹B{¹H} RSHE/MAS-NMRMAS-NMR** (128.4 MHz, 295 K, $\nu_{\text{rot}} = 14.8$ kHz): –37.1 (BCN-Cr) ppm. **¹³C CP/MAS-NMR** (100.6 MHz, 295 K, $\nu_{\text{rot}} = 14.5$ kHz): 236.3–222.3 (br., Cr-CO), 125.8 (br., BCN), 121.4 (br., BCN), 68.9 (OCH₂^{THF}), 26.4 (OCH₂CH₂^{THF}) ppm. **²³Na HPdec/MAS-NMR** (105.8 MHz, 295 K, $\nu_{\text{rot}} = 14.8$ kHz): –14.9 (BCN-Na) ppm. **IR** (ATR [cm^{-1}]): $\nu = 2978$ (w), 2878 (w), 2235 (m, CN), 1912 (vs, CO), 1797 (vs, CO), 1752 (vs, CO), 1487 (w), 1460 (w), 1047 (s), 943 (s), 893 (m), 698 (m), 648 (m), 554 (m), 494 (w), 477 (w). **Raman** (140 mW, [cm^{-1}]): $\nu = 2239$ (vs, CN), 2233 (vs, CN), 1933 (w, CO), 701 (w), 641 (vw), 563 (w), 557 (w), 519 (m), 489 (w), 480 (w).

Synthesis of [PPh₄]₄[{Cr(CO)₃(B(CN)₄)₄}] ([PPh₄]₄[6])

A solution of *fac*-[Cr(CO)₃(MeCN)₃] (60.0 mg, 231.5 μ mol, 1.0 eq.) in THF (5 mL) was treated with a solution of [PPh₄][B(CN)₄] (105.2 mg, 231.5 μ mol, 1.0 eq.) in THF (5 mL) and stirred for 4 hours. The crystalline precipitate was collected by filtration and washed with THF (3 x 5 mL) to produce [PPh₄]₄[{Cr(CO)₃(B(CN)₄)₄}] ([PPh₄]₄[6]) as a yellow solid. Single-crystals suitable for X-ray structure determination were obtained directly out of the reaction mixture when no stirring was applied. **Yield:** 79% (108.1 mg, 45.8 μ mol). **Elemental analysis:** C₁₂₄H₈₀B₄Cr₄N₁₆O₁₂P₄ [2360.31 g/mol] found (calc.): C 62.06 (63.08), H 3.78 (3.42), N 9.15 (9.49)%. **¹¹B{¹H} RSHE/MAS-NMR** (128.4 MHz, 295 K, $\nu_{\text{rot}} = 14.8$ kHz): –37.3 (BCN-Cr) ppm. **¹³C CP/MAS-NMR** (100.6 MHz, 295 K, $\nu_{\text{rot}} = 13.5$ kHz): 229.3 (br., Cr-CO), 135.2 (P-C₆H₅), 130.8 (P-C₆H₅), 126.9 (br., BCN-Cr), 118.6 (P-C₆H₅) ppm. **³¹P CP/MAS-NMR** (162.0 MHz, 295 K): 23.5 (PPh₄) ppm. **IR** (ATR [cm^{-1}]): $\nu = 3060$ (vw), 2224 (m, CN), 1907 (vs, CO), 1779 (vs, CO), 1586 (m), 1484 (m), 1436 (m), 1338 (w), 1189 (w), 1165 (w), 1106 (s), 996(w), 939 m), 751 (w), 720 (s), 686 (s), 641 (s), 522 (w), 523 (vs). **Raman** (140 mW, [cm^{-1}]): $\nu = 3069$ (w), 2232 (s, CN), 2223 (vs, CN), 1929 (m, CO), 1913 (w, CO), 1821 (vw, CO), 1588 (w), 1099 (vw), 1029 (w), 1002 (m), 693 (w), 643 (w), 557 (w), 512 (m), 500 (m).

3 NMR Spectroscopy Section

3.1 General Information

Chemical shifts are listed in parts per million (ppm). Solution NMR spectra were recorded at 298 K using Bruker Avance 400 (^{11}B , 128.5 MHz). ^{11}B NMR spectra were referenced relative to external $\text{BF}_3\cdot\text{OEt}_2$. Solid-state CP/MAS (CP = cross polarization; MAS = magic angle spinning), HPdec/MAS (HPdec = high power decoupling), and RSHE/MAS (RSHE = rotor synchronized hahn echo) NMR spectra were recorded at 293 K with a Bruker Avance NEO 400 NMR spectrometer with bottom layer rotors of ZrO_2 (outer diameter 4 mm with KelF rotor cap) containing approximately 100 μL of sample (ca. 60–130 mg) spinning the rotor at different speeds between 14.5 and 14.8 kHz (^{11}B , 128.4 MHz; ^{13}C 100.6 MHz; ^{23}Na , 105.8 MHz; ^{31}P , 162.0 MHz). All chemical shifts were calibrated externally by setting the ^{13}C low-field signal of adamantine to $\delta = 38.48$ ppm by adjusting the field value of the spectrometer according to the IUPAC recommendations.⁵

3.2 NMR Spectra

$\text{Na}_4[\{\text{Cr}(\text{CO})_3(\text{B}(\text{CN})_4)\}_4]\cdot 6\text{THF}$ ($\text{Na}_4[6]\cdot 6\text{THF}$)

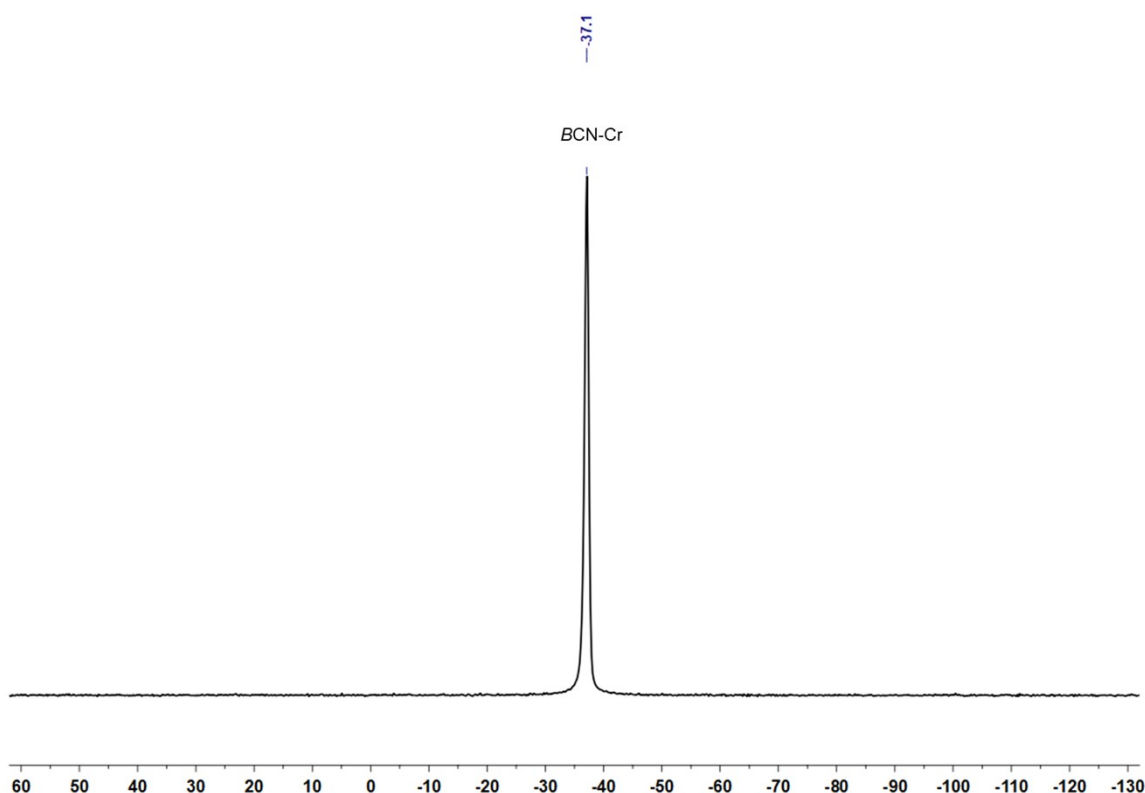


Figure S7. $^{11}\text{B}\{{}^1\text{H}\}$ RSHE/MAS-NMR spectrum $\text{Na}_4[\{\text{Cr}(\text{CO})_3(\text{B}(\text{CN})_4)\}_4]\cdot 6\text{THF}$ ($\text{Na}_4[6]\cdot 6\text{THF}$) ($\nu_{\text{rot}} = 14.8$ kHz).

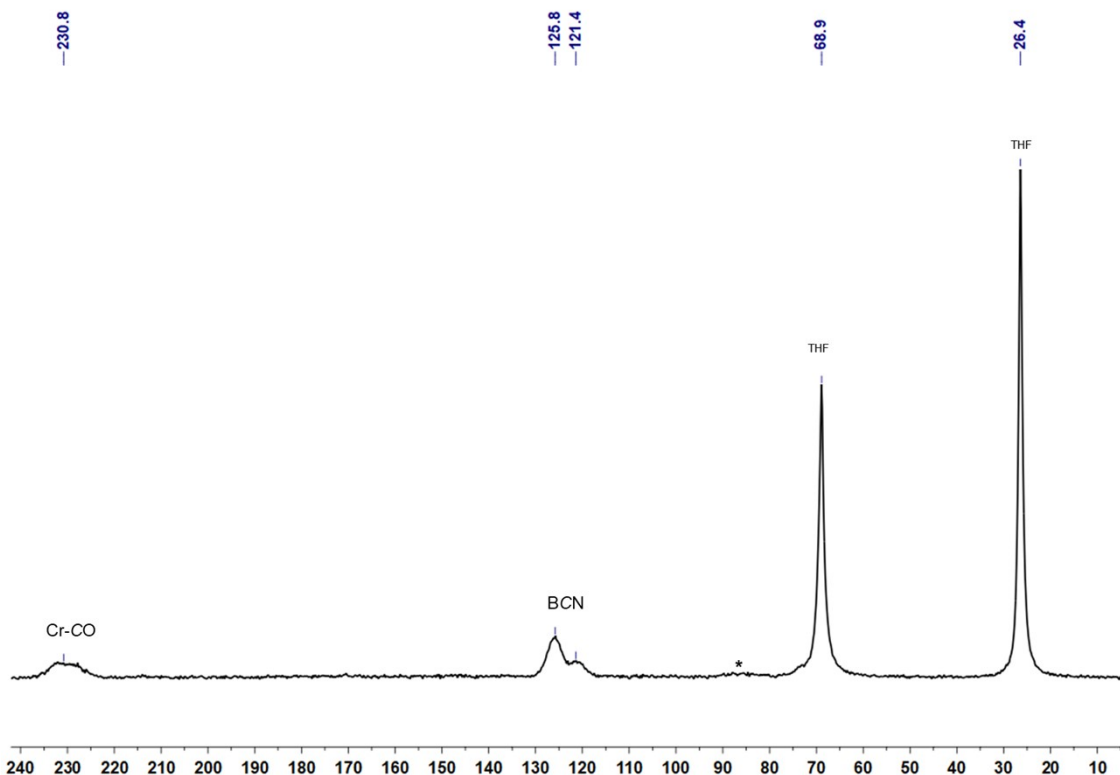


Figure S8. ^{13}C CP/MAS-NMR spectrum of $\text{Na}_4[\{\text{Cr}(\text{CO})_3(\text{B}(\text{CN})_4)\}_4]\cdot 6\text{THF}$ ($\text{Na}_4[6]\cdot 6\text{THF}$) ($\nu_{\text{rot}} = 14.5 \text{ kHz}$). Asterisk (*): Spinning-Sideband.

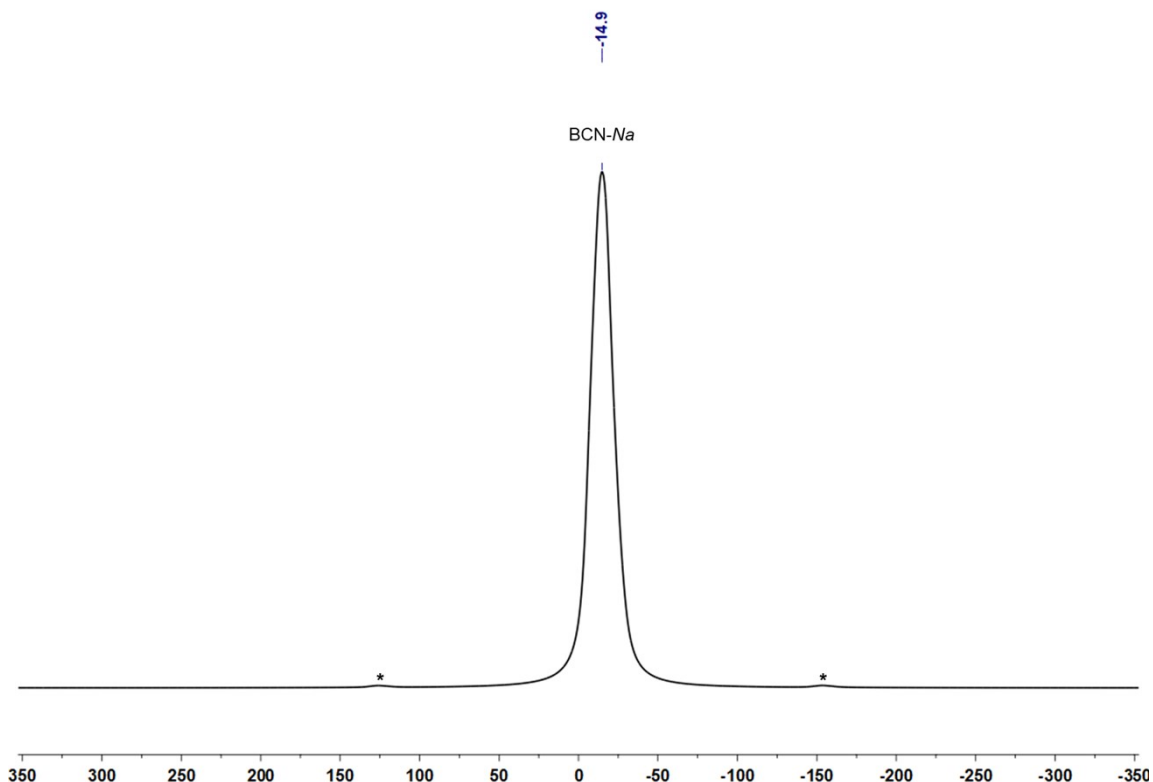


Figure S9. ^{23}Na HPdec/MAS-NMR spectrum of $\text{Na}_4[\{\text{Cr}(\text{CO})_3(\text{B}(\text{CN})_4)\}_4]\cdot 6\text{THF}$ ($\text{Na}_4[6]\cdot 6\text{THF}$) ($\nu_{\text{rot}} = 14.8 \text{ kHz}$). Asterisk (*): Spinning-Sideband.

[PPh₄]₄[{Cr(CO)₃(B(CN)₄)₄}] ([PPh₄]₄[6])

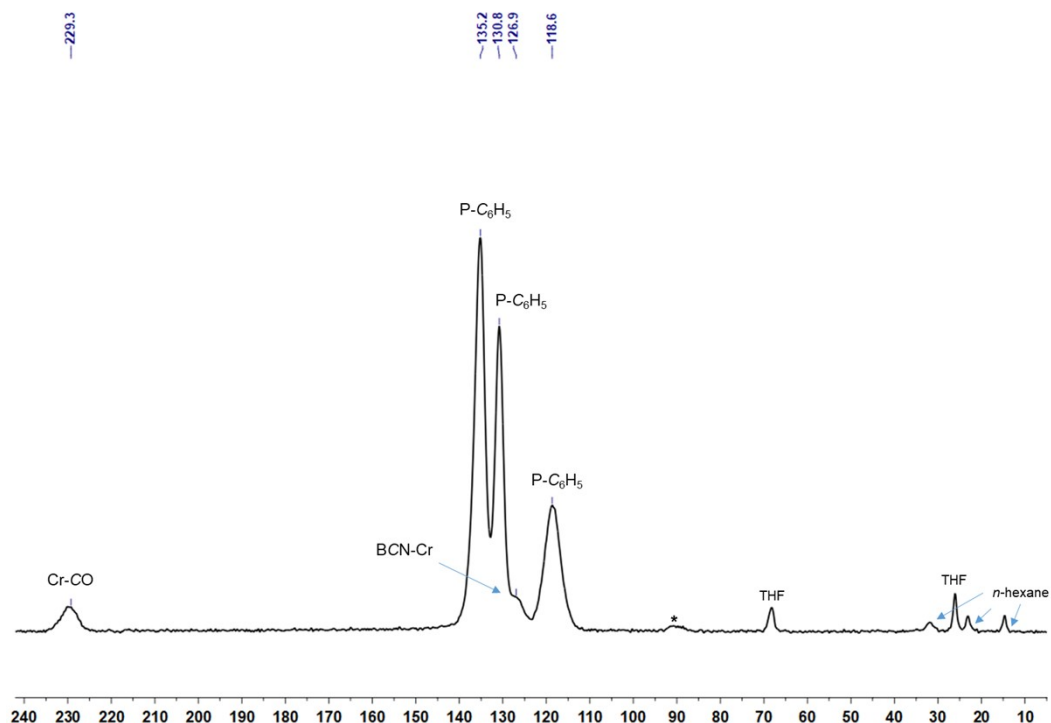


Figure S10. ^{13}C CP/MAS-NMR spectrum of $[\text{PPh}_4]_4[\{\text{Cr}(\text{CO})_3(\text{B}(\text{CN})_4)\}_4]$ ($[\text{PPh}_4]_4[6]$) ($\nu_{\text{rot}} = 14.5 \text{ kHz}$). Asterisk (*): Spinning-Sideband. Despite extensive drying *in vacuo* for multiple days, traces of residual solvents THF and *n*-hexane could not be removed from samples of the product.

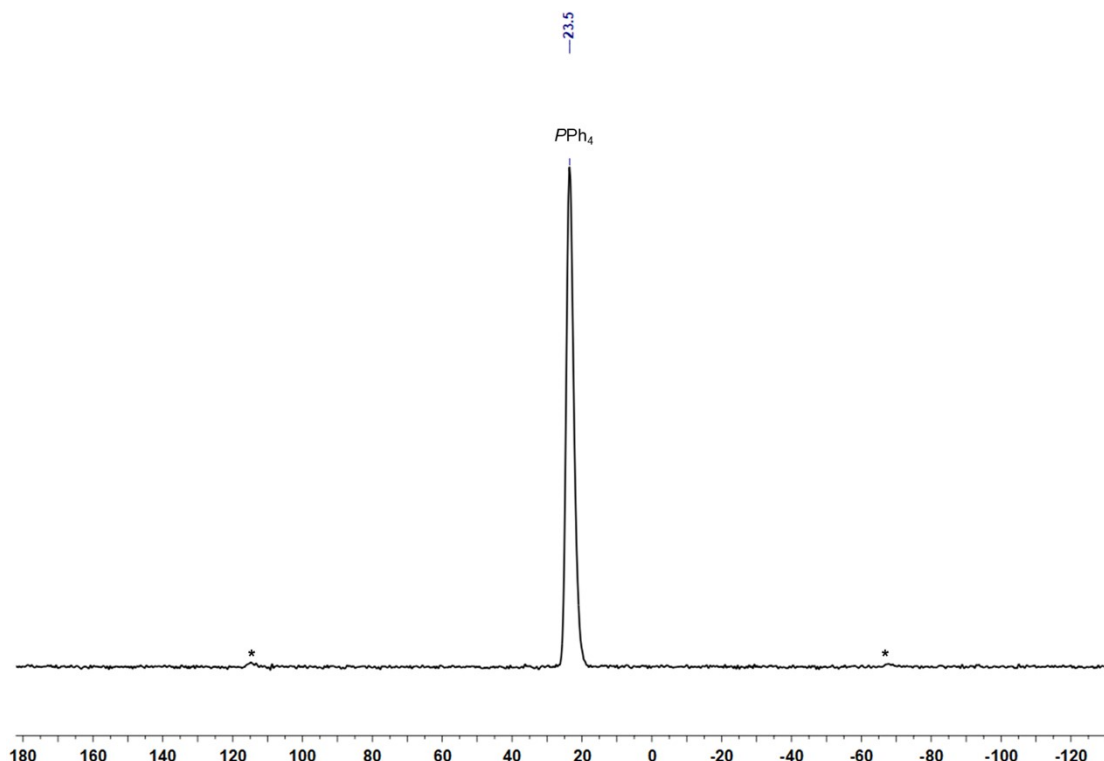


Figure S11. ^{31}P CP/MAS-NMR spectrum of $[\text{PPh}_4]_4[\{\text{Cr}(\text{CO})_3(\text{B}(\text{CN})_4)\}_4]$ ($[\text{PPh}_4]_4[6]$) ($\nu_{\text{rot}} = 14.8 \text{ kHz}$). Asterisk (*): Spinning-Sideband.

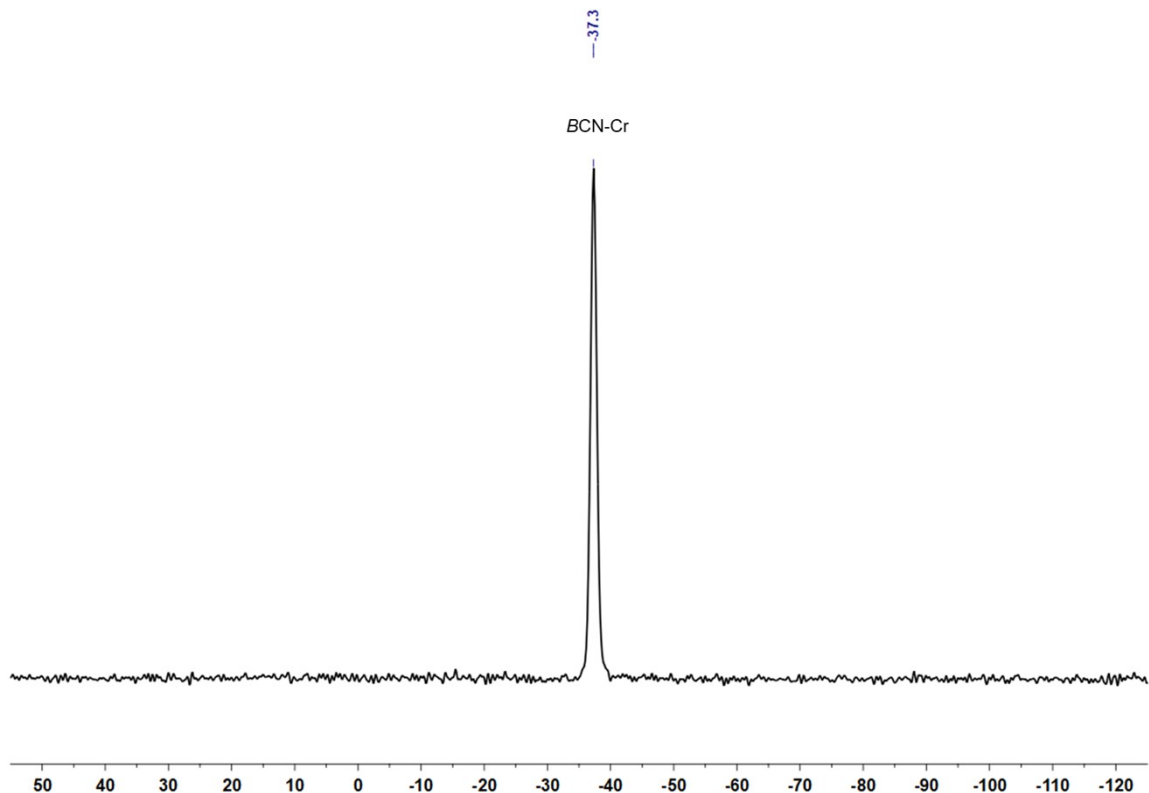


Figure S12. $^{11}\text{B}\{^1\text{H}\}$ RSHE/MAS-NMR spectrum of $[\text{PPh}_4]_4[\{\text{Cr}(\text{CO})_3(\text{B}(\text{CN})_4)\}_4]$ ($[\text{PPh}_4]_4[\mathbf{6}]$) ($\nu_{\text{rot}} = 14.8 \text{ kHz}$).

4 Infrared and Raman Spectroscopy Section

4.1 General Information

Infrared spectra were recorded on a Bruker Alpha I spectrometer as solids by using an ATR unit using 256 scans and a resolution of 4 cm^{-1} . Spectra were plotted using the OPUS software package. Raman spectra were recorded at room temperature with a MultiRAM FT-Raman spectrometer using the 1064 nm excitation line of an Nd/YAG laser on crystalline samples contained in melting point capillaries in the region of $400\text{--}4000\text{ cm}^{-1}$ using a power of 140 mW, 2000 scans and a resolution of 2 cm^{-1} .

4.2 IR and Raman Spectra

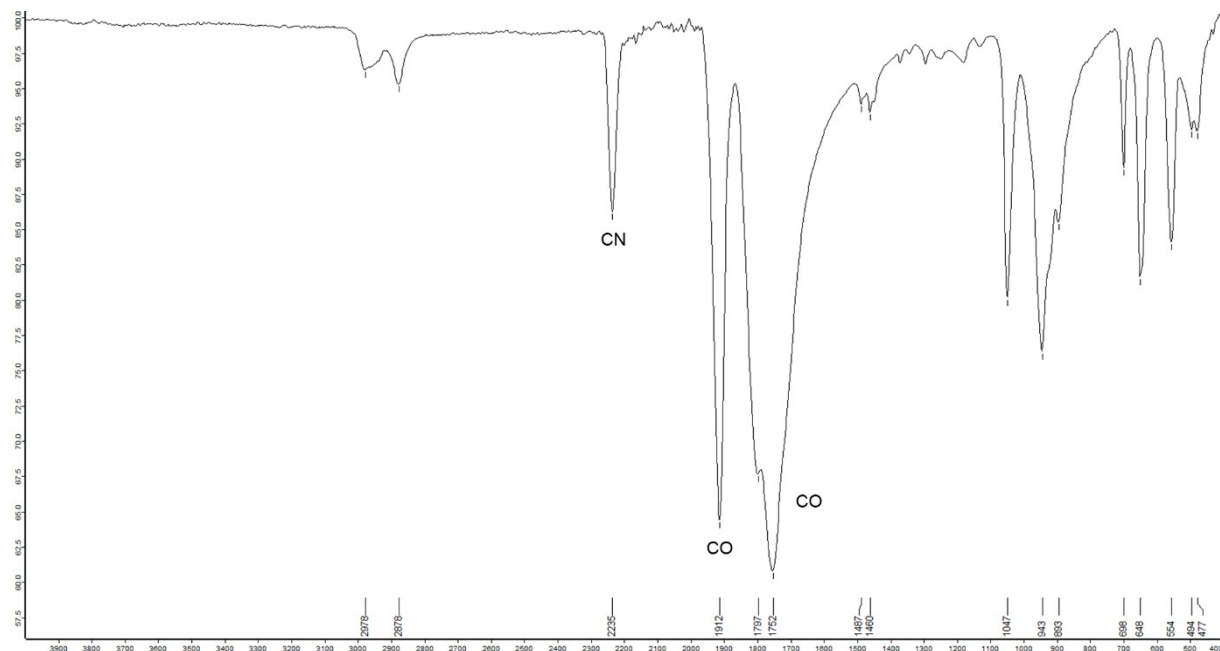


Figure S13. FT-IR spectrum (ATR) of $\text{Na}_4[\text{Cr}(\text{CO})_3(\text{B}(\text{CN})_4)] \cdot 6\text{THF}$ ($\text{Na}_4[6] \cdot 6\text{THF}$)

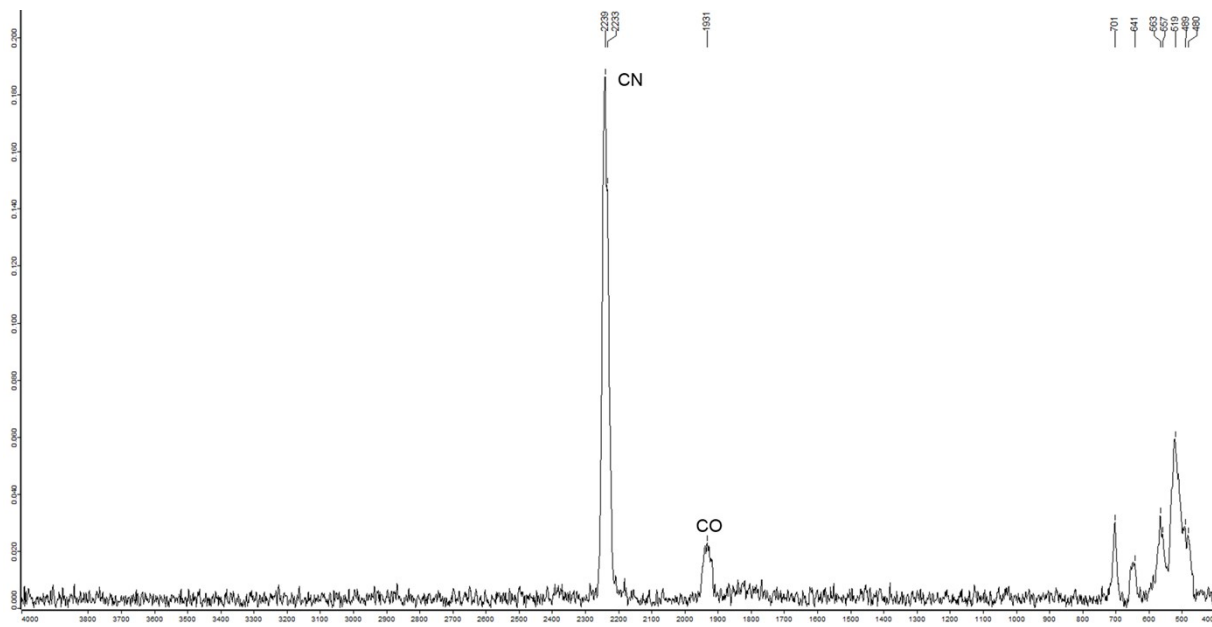


Figure S14. Raman spectrum of $\text{Na}_4[\{\text{Cr}(\text{CO})_3(\text{B}(\text{CN})_4)\}_4]\cdot 6\text{THF}$ ($\text{Na}_4[6]\cdot 6\text{THF}$)

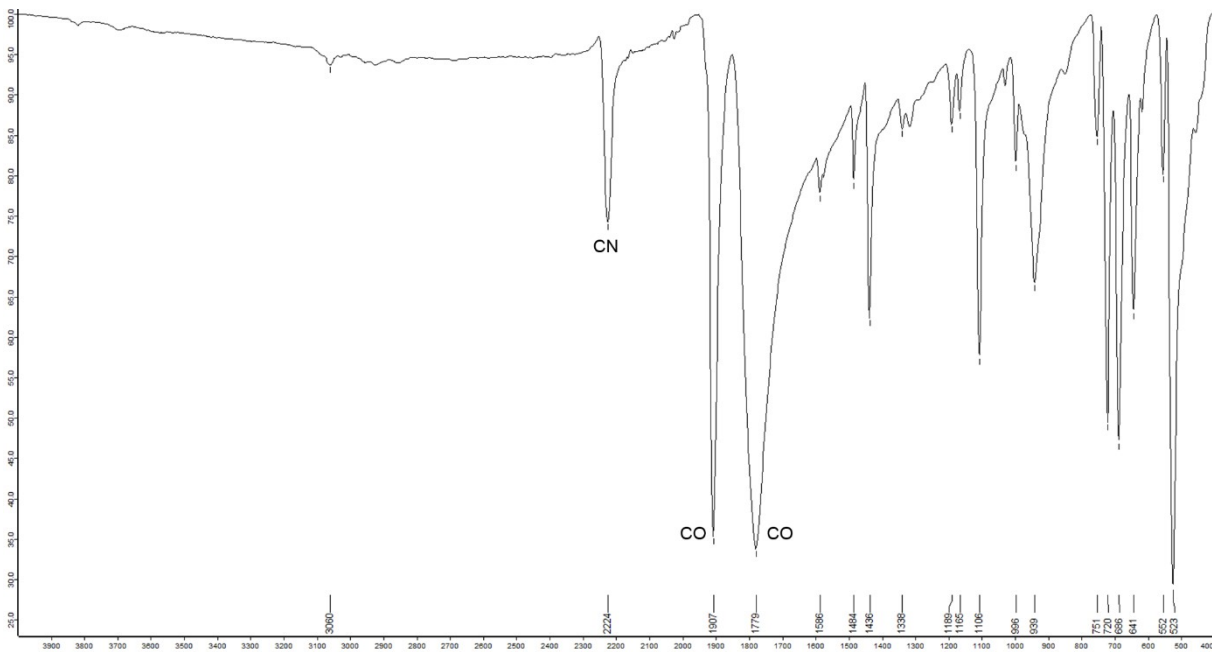


Figure S15. FT-IR spectrum (ATR) of $[\text{PPh}_4]_4[\{\text{Cr}(\text{CO})_3(\text{B}(\text{CN})_4)\}_4]$ ($[\text{PPh}_4]_4[6]$).

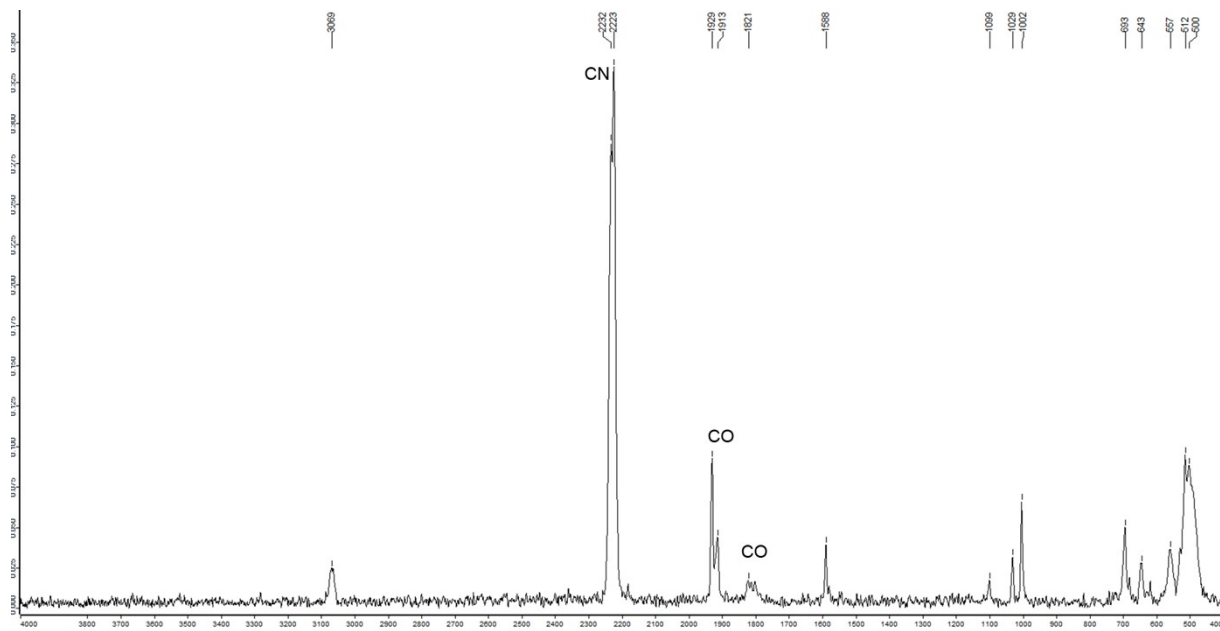


Figure S16. Raman spectrum of $[{\text{PPh}_4}]_4[{\text{Cr}(\text{CO})_3(\text{B}(\text{CN})_4)}_4]$ ($[{\text{PPh}_4}]_4[6]$).

5 Crystallographic Information

5.1 General Information

Crystal data were collected on a Rigaku XtaLAB Synergy Dualflex HyPix diffractometer with a Hybrid Pixel array detector and multi-layer mirror monochromated CuK α radiation equipped with an Oxford Cryo 800 cooling unit. The Crystals were immersed in a film of perfluoropolyether oil on a glass fiber MicroMountTM (MiTeGen) and data were collected at 100 K. The images were processed with the Bruker or Crysaliis software packages and equivalent reflections were merged. Corrections for Lorentz-polarization effects and absorption were performed if necessary and the structures were solved by direct methods. Subsequent difference Fourier syntheses revealed the positions of all other non-hydrogen atoms. The structures were solved by using the ShelXTL software package.⁶ All non-hydrogen atoms were refined anisotropically. Hydrogen atoms were assigned to idealized positions and were included in structure factor calculations. Figures are created using Diamond Crystal and Molecular Structure Visualisation software. Calculations of the Van-der-Waals volumina of the voids inside **6** were performed using the voids tool of the PLATON software package with a grid spacing of 0.2 Å and a probe radius of 1.2 Å.⁷

Crystallographic data (excluding structure factors) for the structures in this paper have been deposited with the Cambridge Crystallographic Data Centre, CCDC, 12 Union Road, Cambridge CB21EZ, UK. Copies of the data can be obtained free of charge on quoting the depository numbers CCDC-2363898 ($\text{Na}(\text{THF})_3[2]$), CCDC-2363899 ($\text{Na}_2(\text{THF})_6[5]\cdot 2\text{THF}$), CCDC-2363900 ($[\text{PPh}_4]_4[6]\cdot 7.5\text{THF}$), and CCDC-2363901 ($\text{Na}_4(\text{THF})_{17}[6]\cdot 2\text{THF}$).

5.2 Crystallographic Data

Crystal data for ${}^1\{\text{Na}(\text{THF})_3[\text{Cr}(\text{CO})_5(\text{B}(\text{CN})_2)]\}$ (${}^1\{\text{Na}(\text{THF})_3[2]\}$):
 $\text{C}_{52}\text{H}_{48}\text{B}_2\text{Cr}_4\text{Na}_2\text{N}_8\text{O}_{26}$, $M_r = 1508.80$ g/mol, $T = 100.00(10)$ K, $\lambda = 1.54184$ Å, yellow block,
 $0.120 \times 0.150 \times 0.210$ mm³, orthorhombic, space group $Pca2_1$, $a = 23.3656(2)$ Å,
 $b = 9.19180(10)$ Å, $c = 31.7925(3)$ Å, $\alpha = 90^\circ$, $\beta = 90^\circ$, $\gamma = 90^\circ$, $V = 6828.14(11)$ Å³, $Z = 4$,
 $\rho_{\text{calcd}} = 1.468$ Mg/m³, $\mu = 6.917$ mm⁻¹, $F(000) = 3072$, 19334 reflections, $0 \leq h \leq 29$, $-11 \leq k \leq 11$, $-39 \leq l \leq 39$, $2.780^\circ < \theta < 77.618^\circ$, completeness 98.8%, 12692 independent reflections,
11864 reflections observed with [$I > 2\sigma(I)$], 940 parameters, 695 restraints, R indices (all data)
 $R_1 = 0.0562$, $wR_2 = 0.1596$, final R indices [$I > 2\sigma(I)$] $R_1 = 0.0530$, $wR_2 = 0.1561$, largest
difference peak and hole 0.715 and -2.180 e Å⁻³, Goof = 1.066.

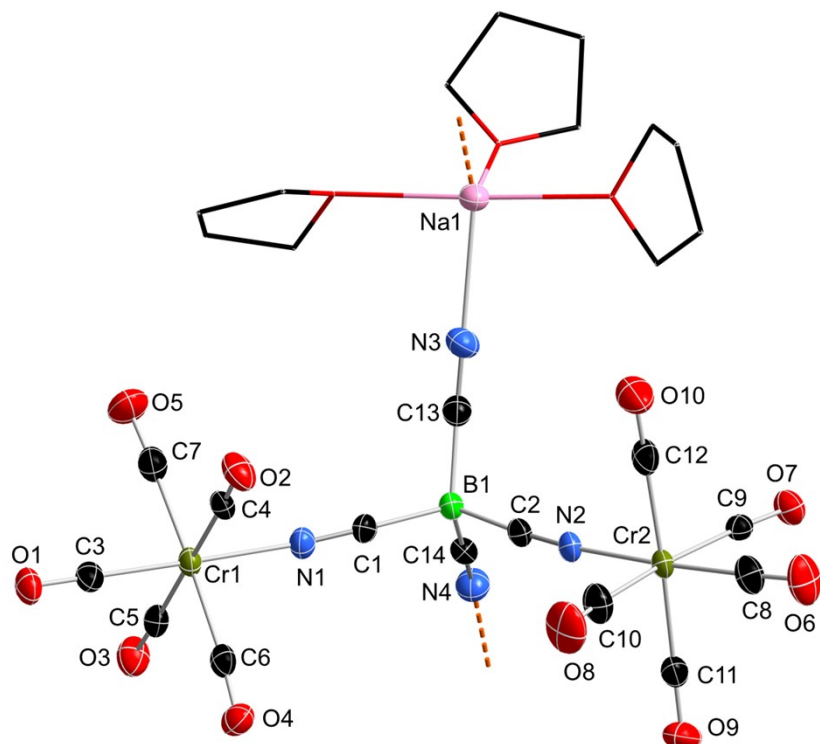


Figure S17. Molecular structure of ${}^1\{\text{Na}(\text{THF})_3[\text{Cr}(\text{CO})_5-\text{NC}]_2\text{B}(\text{CN})_2\}$ (${}^1\{\text{Na}(\text{THF})_3[2]\}$) in the solid-state (ellipsoids set at 50% probability level). The hydrogen atoms are omitted for clarity. Selected bond lengths [Å] and angles [°]: Cr1–N1 2.066(3), Cr2–N2 2.054(4), N1–C1 1.139(5), C1–B1 1.600(5), B1–C2 1.596(6), C2–N2 1.135(6), B1–C13 1.602(6), C13–N3 1.141(6), B1–C14 1.588(6), C14–N4 1.146(5), Na1–N3 2.434(4), Na1–N4' 2.456(4), Cr1–C3 1.860(4), Cr1–C4 1.908(4), Cr1–C5 1.915(5), Cr1–C6 1.925(5), Cr1–C7 1.903(5), C3–O1 1.149(5), C4–O2 1.138(5), C5–O3 1.139(5), C6–O4 1.131(5), C7–O5 1.134(6), Cr2–C8 1.852(5), Cr2–C9 1.917(4), Cr2–C10 1.894(5), Cr2–C11 1.917(4), Cr2–C12 1.911(4), C8–O6 1.150(6), C9–O7 1.138(5), C10–O8 1.147(6), C11–O9 1.135(5), C12–O10 1.133(5), $\angle\text{Cr1N1C1}$ 175.7(3), $\angle\text{N1C1B1}$ 178.6(5), $\angle\text{Cr2N2C2}$ 175.6(3), $\angle\text{N2C2B1}$ 176.2(4).

Crystal data for ${}^3\{\text{Na}_2(\text{THF})_6[\{\text{Cr}(\text{CO})_4(\text{B}(\text{CN})_4)\}_2]\}\cdot 2\text{THF}$ (${}^3\{\text{Na}_2(\text{THF})_6[5]\}\cdot 2\text{THF}$):
 $\text{C}_{24}\text{H}_{32}\text{BCrN}_4\text{NaO}_8$, $M_r = 590.33$ g/mol, $T = 100.00(10)$ K, $\lambda = 1.54184$ Å, yellow block,
 $0.063 \times 0.091 \times 0.234$ mm³, triclinic, space group $P\bar{1}$, $a = 9.8572(4)$ Å, $b = 12.1418(5)$ Å, $c = 12.9109(5)$ Å, $\alpha = 100.325(3)$ °, $\beta = 96.817(3)$ °, $\gamma = 95.944(3)$ °, $V = 1497.08(11)$ Å³, $Z = 2$,
 $\rho_{\text{calcd}} = 1.310$ Mg/m³, $\mu = 3.712$ mm⁻¹, $F(000) = 616$, 9558 reflections, $-12 \leq h \leq 12$, $-13 \leq k \leq 15$, $-16 \leq l \leq 16$, 3.514 ° $< \theta < 74.500$ °, completeness 99.9%, 6095 independent reflections, 5522 reflections observed with [$|I| > 2\sigma(I)$], 539 parameters, 1704 restraints, R indices (all data)
 $R_1 = 0.0809$, $wR_2 = 0.2232$, final R indices [$|I| > 2\sigma(I)$] $R_1 = 0.0758$, $wR_2 = 0.2178$, largest difference peak and hole 0.787 and -0.599 e Å⁻³, Goof = 1.065.

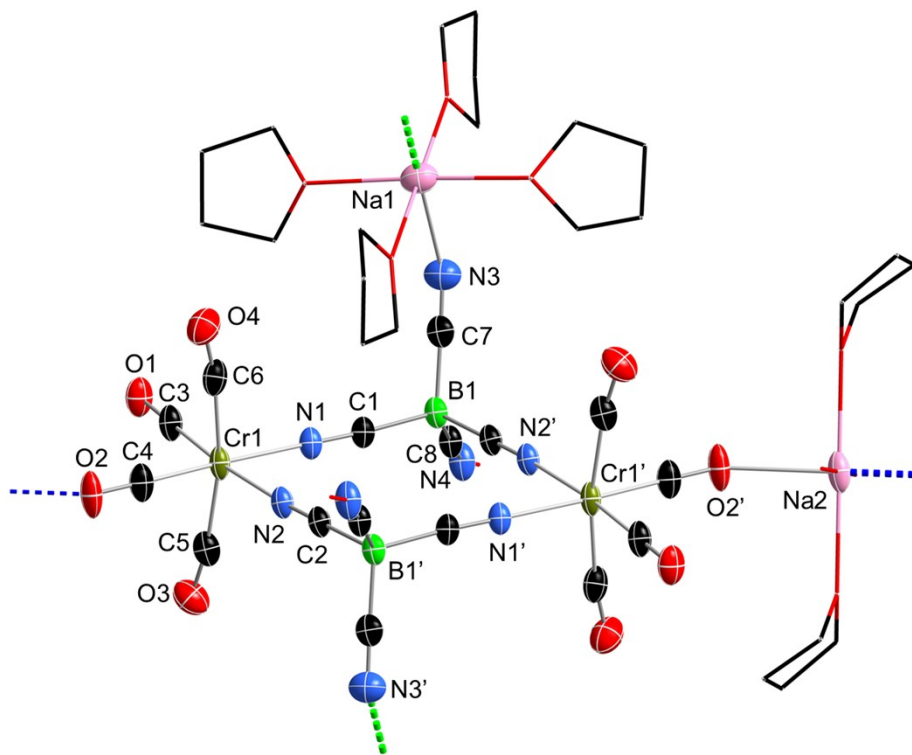


Figure S18. Molecular structure of ${}^3\{\text{Na}_2(\text{THF})_6[\{\text{Cr}(\text{CO})_4(\text{B}(\text{CN})_4)\}_2]\}\cdot 2\text{THF}$ (${}^3\{\text{Na}_2(\text{THF})_6[5]\}\cdot 2\text{THF}$): in the solid-state (ellipsoids set at 35% probability level). The hydrogen atoms not bound at boron are omitted for clarity. Selected bond lengths [Å] and angles [°]: Cr1–N1 2.062(3), N1–C1 1.144(4), C1–B1 1.587(5), B1–C2' 1.595(5), C2–N2 1.141(4), N2–Cr1 2.064(3), B1–C7 1.589(5), B1–C8 1.598(6), C7–N3 1.134(4), C8–N4 1.125(5), Cr1–C3 1.853(4), Cr1–C4 1.830(4), Cr1–C5 1.898(4), Cr1–C6 1.927(4), C3–O1 1.151(5), C4–O2 1.156(5), C5–O3 1.143(5), C6–O4 1.138(5), Na1–O2 2.390(3), N3–Na1 2.430(3), N4–Na2 2.456(3), $\angle \text{Cr1N1C1}$ 176.1(2), $\angle \text{N1C1B1}$ 174.8(3), $\angle \text{Cr1N2C2}$ 176.2(3), $\angle \text{N2C2B1'}$ 177.5(3), $\angle \text{N1Cr1N2}$ 82.5(1), $\angle \text{Cr1C5O3}$ 171.5(3), $\angle \text{Cr1C6O4}$ 171.9(4), $\angle \text{C1B1C2'}$ 108.5(3), $\angle \text{N1Cr1N2}$ 82.5(1).

Crystal data for $\text{^2}\{\text{Na}_4(\text{THF})_{17}[\{\text{Cr}(\text{CO})_3(\text{B}(\text{CN})_4)\}_4]\}\cdot\text{2THF}$ ($\text{^2}\{\text{Na}_4(\text{THF})_{17}[6]\}\cdot\text{2THF}$):
 $\text{C}_{104}\text{H}_{152}\text{B}_4\text{Cr}_4\text{N}_{16}\text{Na}_4\text{O}_{31}$, $M_r = 2465.61$ g/mol, $T = 100.00(10)$ K, $\lambda = 1.54184$ Å, yellow block, $0.370 \times 0.230 \times 0.180$ mm³, monoclinic, space group $P2_1/n$, $a = 17.5473(2)$ Å, $b = 20.8549(2)$ Å, $c = 35.3881(3)$ Å, $\alpha = 90^\circ$, $\beta = 102.200(1)^\circ$, $\gamma = 90^\circ$, $V = 12657.7(2)$ Å³, $Z = 4$, $\rho_{\text{calcd}} = 1.294$ Mg/m³, $\mu = 3.530$ mm⁻¹, $F(000) = 5184$, 227094 reflections, $-21 \leq h \leq 21$, $-23 \leq k \leq 25$, $-42 \leq l \leq 43$, $2.474^\circ < \theta < 71.679^\circ$, completeness 98.7%, 24444 independent reflections, 20989 reflections observed with [$I > 2\sigma(I)$], 1974 parameters, 6648 restraints, R indices (all data) $R_1 = 0.0912$, $wR_2 = 0.2145$, final R indices [$I > 2\sigma(I)$] $R_1 = 0.0806$, $wR_2 = 0.2065$, largest difference peak and hole 0.983 and -0.759 e Å⁻³, Goof = 1.056.

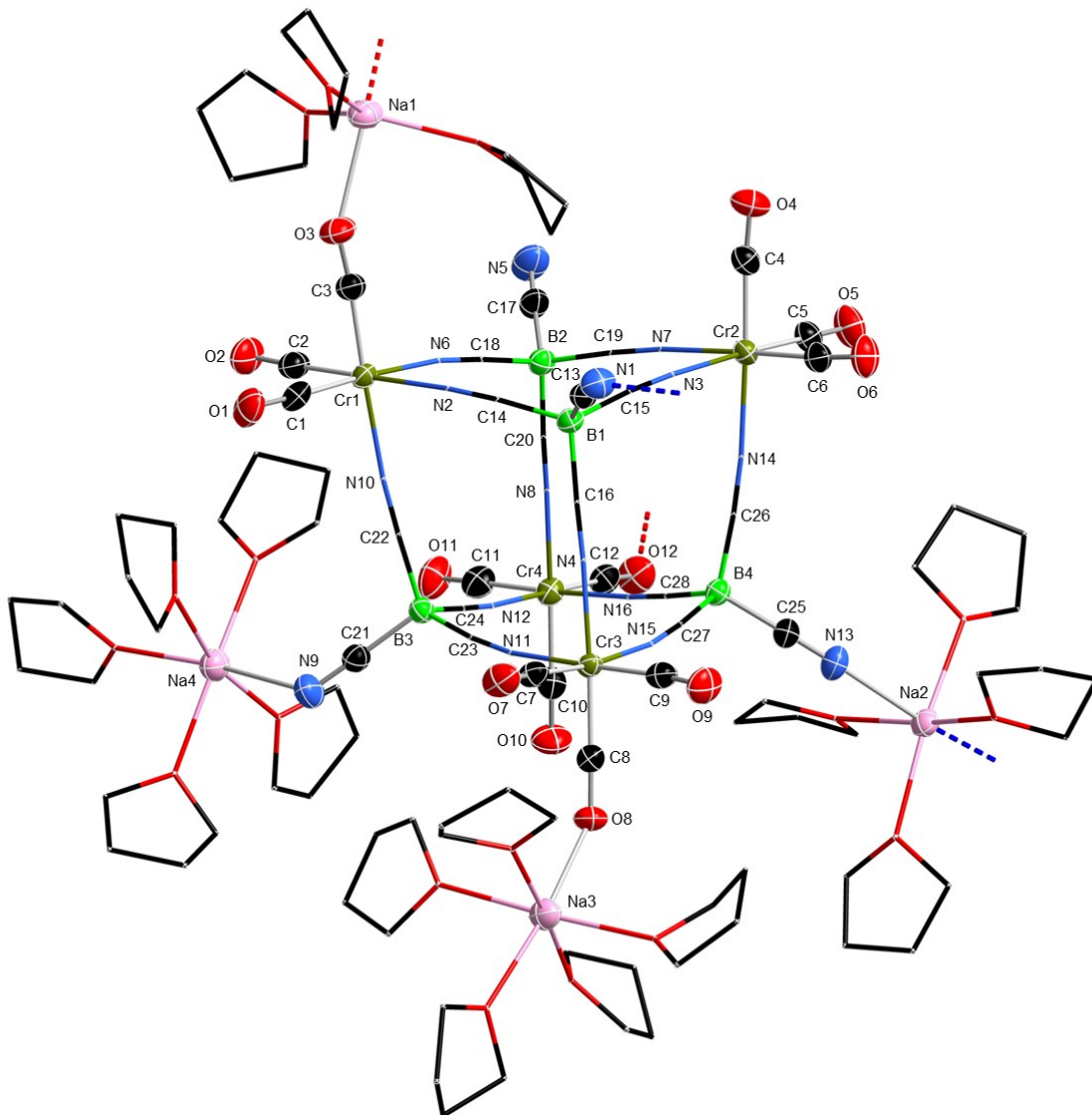


Figure S19. Solid-state structure of the central motif in $\text{^2}\{\text{Na}_4(\text{THF})_{17}[\{\text{Cr}(\text{CO})_3(\text{B}(\text{CN})_4)\}_4]\}\cdot\text{2THF}$ ($\text{^2}\{\text{Na}_4(\text{THF})_{17}[6]\}\cdot\text{2THF}$) in the solid-state (ellipsoids set at 50% probability level). Only half of the asymmetric unit is shown for clarity. The hydrogen atoms and non-coordinated co-crystallized THF molecules are also omitted for clarity. Some of the THF molecules also showed 2-fold disorder, only the part with the greater occupation is shown. Selected bond lengths [Å] and angles [°]: Cr1–C1 1.826(4),

C1–O1 1.174(5), Cr1–C2 1.831(4), C2–O2 1.169(5), Cr1–C3 1.819(4), C3–O3 1.174(5), Cr2–C4 1.830(4), C4–O4 1.164(5), Cr2–C5 1.832(4), C5–O5 1.17085), Cr2–C6 1.83384), C6–O6 1.162(59, Cr3–C7 1.836(4), C7–O7 1.166(5), Cr3–C8 1.817(4), C8–O8 1.175(5), Cr3–C9 1.842(4), C9–O9 1.157(5), Cr4–C10 1.845(4), C10–O10 1.160(5), Cr4–C11 1.827(5), C11–O11 1.167(5), Cr4–C12 1.811(4), C12–O12 1.177(5), Cr1–N2 2.083(3), Cr1–N6 2.076(3), Cr1–N10 2.081(3), Cr2–N3 2.064(3), Cr2–N7 2.068(3), Cr2–N14 2.072(3), Cr3–N4 2.063(3), Cr3–N11 2.062(3), Cr3–N15 2.075(3), Cr4–N8 2.078(3), Cr4–N12 2.068(4), Cr4–N16 2.083(3), Na1–O3 2.360(3), Na2–N13 2.469(4), Na3–O8 2.435(3), Na4–N9 2.543(4), <N2Cr1N6 83.85(12), <N2Cr1N10 82.20(12), <N6Cr1N10 83.05(12), <N3Cr2N7 82.23(12), <N3Cr2N14 83.28(12), <N7Cr2N14 83.68(12), <N11Cr3N15 83.09(12), N4Cr3N15 82.70(12), N4Cr3N11 82.33(12), <N8Cr4N12 82.80(13), <N8Cr4N16 83.25(12), N12Cr4N16 81.90(13), <C1Cr1C2 84.97(19), <C1Cr1C3 86.31(19), <C2Cr1C3 87.17818), <C4Cr2C5 89.39(18), <C4Cr2C6 85.74(18), <C5Cr2C6 87.04(17), <C7Cr3C88 8.01(17), <C8Cr3C9 85.85(17), <C7Cr3C9 86.49(19), <C10Cr4C11 87.35(18), <C10Cr4C12 85.67(18), <C11Cr4C12 86.14(19).

Crystal data for $[\text{PPh}_4]_4[\{\text{Cr}(\text{CO})_3(\text{B}(\text{CN})_4)\}_4] \cdot 7.5\text{THF}$ ($[\text{PPh}_4]_4[6] \cdot 7.5\text{THF}$):
 $\text{C}_{154}\text{H}_{140}\text{B}_4\text{Cr}_4\text{N}_{16}\text{O}_{19.5}\text{P}_4$, $M_r = 2901.93$ g/mol, $T = 100.00(10)$ K, $\lambda = 1.54184$ Å, yellow block, $0.180 \times 0.090 \times 0.050$ mm³, triclinic, space group $P\bar{1}$, $a = 16.60540(10)$ Å, $b = 18.2464(2)$ Å, $c = 27.5141(2)$ Å, $\alpha = 93.2220(10)$ °, $\beta = 99.5440(10)$ °, $\gamma = 113.6920(10)$ °, $V = 7458.23(12)$ Å³, $Z = 2$, $\rho_{\text{calcd}} = 1.292$ Mg/m³, $\mu = 3.299$ mm⁻¹, $F(000) = 3016$, 140144 reflections, $-20 \leq h \leq 20$, $-22 \leq k \leq 23$, $-30 \leq l \leq 34$, 2.669 ° < θ < 77.387 °, completeness 99.2%, 30626 independent reflections, 24937 reflections observed with $|I| > 2\sigma(I)$, 2519 parameters, 4199 restraints, R indices (all data) $R_1 = 0.0897$, $wR_2 = 0.2164$, final R indices $|I| > 2\sigma(I)$ $R_1 = 0.0749$, $wR_2 = 0.2032$, largest difference peak and hole 1.617 and -0.930 e Å⁻³, Goof = 1.010.

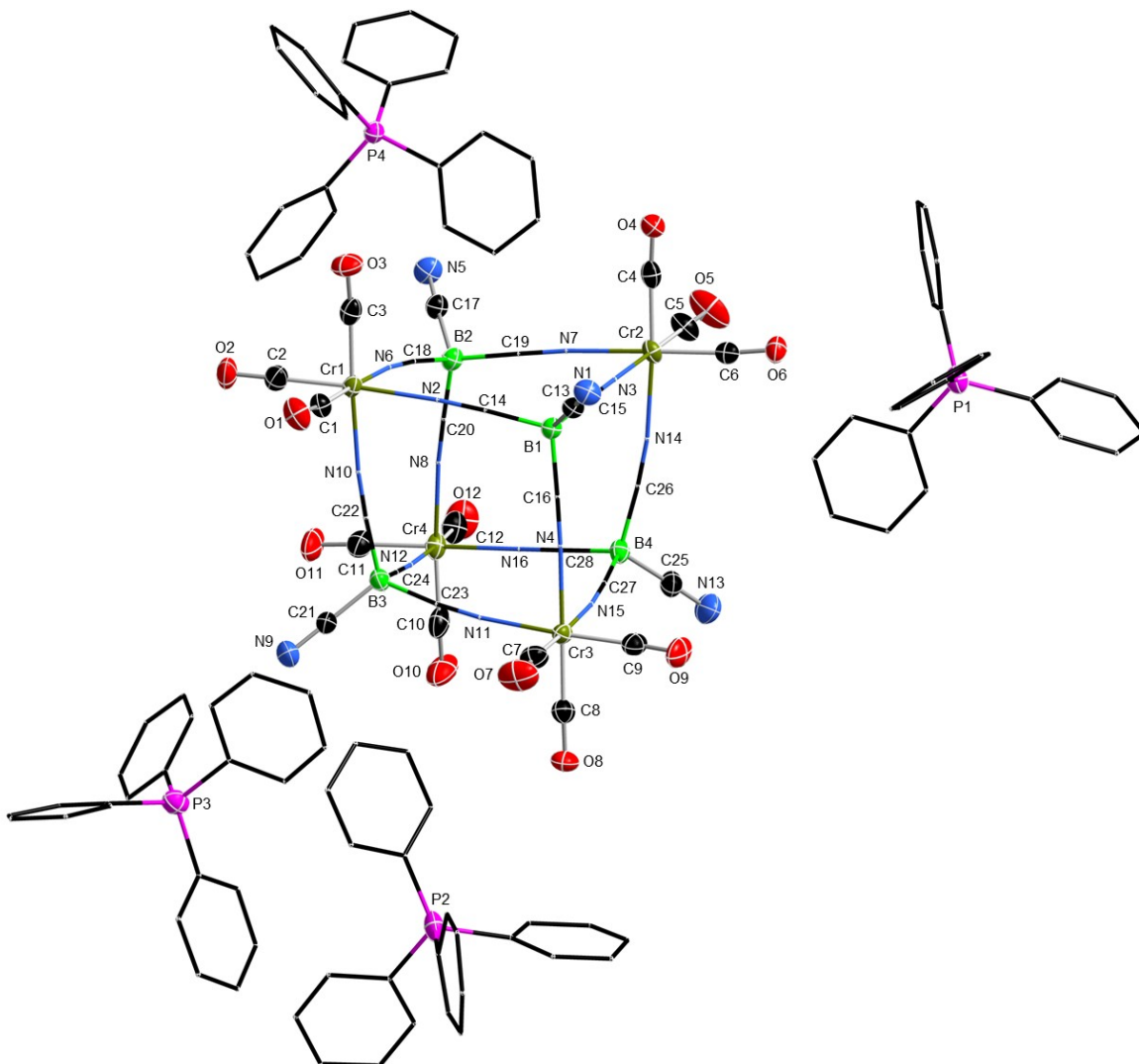


Figure S20. Solid-state structure of the central motif in $[\text{PPh}_4]_4[\{\text{Cr}(\text{CO})_3(\text{B}(\text{CN})_4)\}_4] \cdot 7.5\text{THF}$ ($[\text{PPh}_4]_4[6] \cdot 7.5\text{THF}$) in the solid-state (ellipsoids set at 50% probability level). The hydrogen atoms and non-coordinated co-crystallized THF molecules are omitted for clarity. Selected bond lengths [Å] and angles [°]: Cr1–C1 1.834(4), C1–O1 1.161(4), Cr1–C2 1.836(4), C2–O2 1.166(5), Cr1–C3 1.838(4), C3–O3 1.170(5), Cr2–C4 1.841(4), C4–O4 1.162(5), Cr2–C5 1.829(4), C5–O5 1.161(5), Cr2–C6 1.830(4), C6–O6 1.168(4), Cr3–C7 1.820(4), C7–O7 1.158(5), Cr3–C8 1.846(4), C8–O8 1.158(5), Cr3–C9 1.824(4), C9–O9 1.172(5), Cr4–C10 1.830(5), C10–O10 1.162(5), Cr4–C11 1.831(4), C11–O11

1.164(5), Cr4—C12 1.834(4), C12—O12 1.169(5), Cr1—N2 2.072(3), Cr1—N6 2.093(3), Cr1—N10 2.080(3), Cr2—N1 2.067(3), Cr2—N7 2.076(3), Cr2—N14 2.084(3), Cr3—N4 2.072(3), Cr3—N11 2.067(3), Cr3—N15 2.079(3), Cr4—N8 2.064(3), Cr4—N12 2.063(3), Cr4—N16 2.090(3), <N2Cr1N6 83.4(1), <N2Cr1N10 83.1(1), <N6Cr1N10 83.4(1), <N1Cr2N7 82.5(1), <N1Cr2N14 84.0(1), <N7Cr2N14 82.5(1), <N4Cr3N11 83.3(1), <N4Cr3N15 83.0(1), <N11Cr3N15 84.9(1), <N8Cr4N12 83.0(1), <N8Cr4N16 82.7(1), <N12Cr4N16 84.3(1), <C1Cr1C2 84.4(2), <C1Cr1C3 84.9(2), <C2Cr1C3 89.1(2), <C4Cr2C5 86.8(2), <C4Cr2C6 87.0(2), <C5Cr2C6 83.7(2), <C7Cr3C8 86.4(2), <C7Cr3C9 86.4(2), <C8Cr3C9 87.6(2), <C10Cr4C11 89.0(2), <C10Cr4C12 87.0(2), <C11Cr4C12 85.9(2).

6 Author Contributions

M. S. L., U. R. and M. F. conceived of the project and wrote the manuscript. M. S. L. and R. B. performed analytical measurements. M. S. L. synthesized the compounds.

7 References

1. J. Attner and U. Radius, *Chem. Eur. J.*, 2001, **7**, 783-790.
2. L. A. Bischoff, M. Drisch, C. Kerpen, P. T. Hennig, J. Landmann, J. A. P. Sprenger, R. Bertermann, M. Grune, Q. Yuan, J. Warneke, X. B. Wang, N. V. Ignat'ev and M. Finze, *Chem. Eur. J.*, 2019, **25**, 3560-3574.
3. A. Flemming, M. Hoffmann and M. Köckerling, *Z. Anorg. Allg. Chem.*, 2010, **636**, 562-568.
4. D. P. Tate, W. R. Knipple and J. M. Augl, *Inorg. Chem.*, 1962, **1**, 433-434.
5. R. K. Harris, E. D. Becker, S. M. C. d. Menezes, R. Goodfellow and P. Granger, *Pure Appl. Chem.*, 2001, **73**, 1795-1818.
6. G. M. Sheldrick, *Acta Crystallogr. Sect. C Struct. Chem.*, 2015, **71**, 3-8.
7. A. L. Spek, *J. Appl. Cryst.*, 2003, **36**, 7-11.